

Peri-Implant Bone Organization under Immediate Loading Conditions: Collagen Fiber Orientation and Mineral Density Analyses in the Minipig Model

Tonino Traini, DDS, PhD;* Jörg Neugebauer, DDS;† Ulf Thams, MD, DDS;‡ Joachim E. Zöller, MD, DDS, PhD;† Sergio Caputi, MD, DDS;* Adriano Piattelli, MD, DDS*

ABSTRACT

Background: Mechanical properties of bones are greatly influenced by percentages of organic and mineral constituents. Nevertheless, information about mineralization level on a microscopic scale and collagen fiber organization in peri-implant bone after immediate loading is scarce.

Purpose: The aim of this work was to analyze and compare the degree of mineralization and collagen fiber orientation in alveolar bone (AB) and peri-implant bone of immediately loaded (IL) and unloaded (NL) implants.

Materials and Methods: A total of 25 dental implants of 3.8 mm in diameter and 11 mm in length were used in the present study. In five minipigs, three premolars and the first molar were removed from the left side of the mandible. Three months later, five implants for each animal were inserted. Four implants were loaded immediately with a fixed restoration, while one implant was left unloaded. After a 4-month healing period, all implants were retrieved. Circularly polarized light and scanning electron microscope with backscattered electron imaging were used to analyze both peri-implant and AB retrieved 5 mm from the implant.

Results: The bone/implant contact ratio (BIC %) was $77.8 \pm 5.9\%$ for the IL implants and $78.0 \pm 5.8\%$ for the NL implants; the difference was not statistically significant ($p = 0.554$). In the peri-implant bone, the area related to transverse collagen fibers was $112,453 \pm 4,605$ pixels for IL implants and $87,256 \pm 2,428$ pixels for NL implants. In the AB, the area related to transverse collagen fibers was $172,340 \pm 3,892$ pixels. The difference between groups was statistically significant ($p < .001$). The degree of mineralization of peri-implant bone was 137 ± 19 gray level for IL implants and 115 ± 24 gray level for NL implants, while in the AB, the degree of mineralization was 125 ± 26 gray level. This difference was statistically significant ($p < .001$).

Conclusion: In this study, it was found that IL and NL implants showed the same degree of osseointegration. The bone matrix around IL implants had a higher quantity of transverse collagen fibers and presented a higher level of mineralization.

KEY WORDS: birefringence circularly polarized light, collagen fiber orientation, dental implants, immediate loading, osseointegration, backscattered electron imaging, mineral content, mineral density

INTRODUCTION

Implant surface plays an important role for both osseointegration and bone matrix mineralization¹; the double-etched surface treatment decreases the healing time to 8 weeks,² while the sandblasted acid-etched surface decreases the healing time to 6 weeks.³ The micro-textured surface of the implants improves the “de novo” bone formation due to the early adhesion of non-collagen proteins, like plasma proteins, during the clot phase and later on with osteopontin and bone sialoprotein. The mineralization of the bone matrix

*Dental School, University of Chieti-Pescara, Italy; †Department of Craniomaxillofacial and Plastic Surgery, University of Cologne, Cologne, Germany; ‡Private Practice, Madrid, Spain

Reprint requests: Professor Adriano Piattelli, MD, DDS, Via F. Sciucchi 63 66100 Chieti, Italy; e-mail: apiattelli@unich.it

© 2008, Copyright the Authors

Journal Compilation © 2008, Wiley Periodicals, Inc.

DOI 10.1111/j.1708-8208.2008.00086.x

starts with calcium phosphate nucleation at the calcium binding sites on these proteins and continues by crystal growth and collagen production until it completes osseointegration.¹ A histological study in rabbits showed that the micro-fractures, which occur due to the bone condensing technique, improve the peri-implant bone formation in the first weeks by the release of cytokines.⁴ It is well established that small adjustments in mineral content can significantly affect the mechanical properties of bone.^{5,6} Furthermore, in bone tissue, the distribution of the mineral depends on the rate of the bone turnover. A high turnover rate results in a large difference in mineral content between the interstitial bone and the surface layer. Increasing mineralization density increases the strain resistance of bone. However, it has been demonstrated in femoral cortical bone that with an ash content above 60% by weight, there is a decreasing ability to absorb impact energy.⁶ The microscopic variation of mineral contents in bone is difficult to measure. Micro-radiography (MR) has been developed to evaluate the mineral content at the microscopic level in thin sections⁷; however, the resolution of MR, which ranges from 400 to 4000 μm^3 , is limited by errors caused by projection effects. Furthermore, the necessity to collect a large number of specimens, ground or milled to a uniform thickness of 100 μm , is difficult to accomplish.⁸ Backscattered electron (BSE) evaluation has important advantages in terms of volume resolution and circumvents these problems since the volumetric resolution ranged from 0.07 to 137 μm^3 .⁹ The BSE has been successfully applied by Skedros and colleagues¹⁰ to study the mineral content and the composition of bone in plastic-embedded specimens. The use of BSE imaging to determine mineral content is based on the well-established principle that the fraction of electrons collides with a target sample leaving it again as BSEs to form the image. According to classical histology, bone tissue may be classified in relation to the spatial orientation of collagen fibers. Two different types of bone have been recognized: woven-fibered bone and parallel-fibered bone (lamellar or non-lamellar). Woven bone has a poorly structured matrix that is formed rapidly in response to wounding or hypertrophic adaptation. The slower the appositional rate, the more highly organized the matrix and the greater the strength of the bone; the degree of stiffness and strength of a bone is also related to mineralization.^{5,6} The presence of collagen in the bone matrix is important for how much energy is required to cause matrix fail-

ure.¹¹ A study in human femoral specimens has demonstrated that transversely oriented collagen fibers are more prevalent in bone areas that are known to undergo compression, while predominantly longitudinally oriented collagen fibers are prevalent in those that undergo tension.¹² These findings thus suggest that collagen fiber orientation is a strong predictor of a bone loading regimen. Circularly polarized light (CPL) was used as a standard investigation method due to the fact that bone shows birefringence dependent upon the orientation of its collagen fibers.^{13,14} This minipig study was performed to characterize both mineralization degree and collagen fiber organization of the bone matrix to evaluate the overall quality of osseointegration in immediately loaded (IL) and unloaded (NL) dental implants compared to the alveolar bone (AB).

MATERIALS AND METHODS

The study protocol was approved by the Institutional Animal Care Committee of the Military Hospital "General Gomez-Roman" Madrid, Spain. Five adult Göttingen minipigs (18–21 months of age, average weight 35 kg) were used in the present study. The three premolars and the first molar were removed from the left side of the mandible of each animal under general anesthesia which was maintained by halothane 2% in an oxygen/nitrous oxide mixture (1/1) (Linde AG, Höllriegelskreuth, Germany). To secure normal blood gases, the animals were artificially ventilated with a volume per minute of 150 mL/kg body weight/min. After achieving anesthesia, before the removal of the teeth, impressions of the dentition were taken from the left side of the mandible (Impregum™ Penta™, ESPE Dental AG, Seefeld, Germany) to fabricate vacuum-formed templates for the prosthetic supply. After a healing period of 3 months, the implant placement was performed under general anesthesia. The mucosa was rinsed with 0.2% chlorhexidine gluconate (Doreperol®N, Dr. Rentschler Arzneimittel GmbH & Co., Laupheim, Germany); the implant sites were sequentially enlarged to 3.8 mm in diameter with pilot and spiral drills according to the standard protocol of the manufacturer (XiVE®Plus, Dentsply-Friadent GmbH, Mannheim, Germany). The bone implant bed was prepared for a depth of 5 mm. This procedure performed a standardized undersized preparation to achieve a higher mechanical stabilization. Each animal received five cylindrical, self-tapping screw implants of 3.8 mm in diameter and 11 mm in length

TABLE 1 Summary of the Parameters Considered in the Study

No. of Specimens	No. of Sections	No. of Measurements for BSE	No. of Measurements for CPL	No. of Measurements for Section	No. of Measurements for Specimen	Site of Measure
IL 20	40	200	200	5	10	Until 1 mm from implant
AB 20	40	200	200	5	10	All the imaged area
NL 5	10	50	50	5	10	Until 1 mm from implant

AB = alveolar bone; BSE = backscattered electrons; CPL = circularly polarized light; IL = immediately loaded implants; NL = unloaded implants.

(XiVE Plus). The threads of the dental implant used were of different sizes: about 0.25 mm in section for the first four coronal threads and 0.75 mm in section for the apical threads. A total of 25 implants were placed. The wound closure was carried out with resorbable sutures (Vicryl® 2-0, Ethicon GmbH, Norderstedt, Germany). For each animal, the proximal implants were left unloaded (NL), while the four distal implants were immediately loaded (IL), receiving fiber-reinforced bridges at the end of surgery. The bridges were placed on four implants, while the interimplant distance was of about 2 mm. Prefabricated temporary abutment caps (Palavit® G, Haereus Kulzer GmbH, Wehrheim, Germany) were positioned on the temporary abutments. Fiber-reinforced strips (Fibrekor®, Jeneric®/Pentron® Inc., Wallingford, CT, USA) were used to connect the temporary abutment caps. The vacuum-formed templates were filled with temporary acrylic (Protemp®Garant, ESPE Dental AG) and were positioned over the temporary abutment caps. Saline irrigation was used to cool the resin during the polymerization period. Subsequently, the supra-structure was removed and contoured. The interproximal spaces were opened by 2 mm to prevent pressure on the mucosa during the postoperative swelling. The bridges were installed with Harvard Cement (Richter & Hoffmann Dental-Gesellschaft, Berlin, Germany). The seating of the restorations was checked by palpating the margins with an explorer through the soft extruded cement. Once the cement had completely set, all the excess cement was removed by means of scalers, explorers, and knotted dental floss. The gingival crevice was checked with an explorer several times to ensure that all the cement had been removed. Occlusal interferences were evaluated intraorally with 20- μ m-thick occlusal articulating paper. The occlusal contacts were checked by hand manipulating the mandible so that mandibular

and maxillary teeth were tapped together, the marks made by the articulating ribbon were adjusted to reach very light contacts on the restorations. After surgical and prosthetic procedure, an antibiotic was administered subcutaneously (benzylpenicilline/dihydrostreptomycine, Tardomycel®, BayerVital GmbH, Leverkusen, Germany; 0.5 mL every 48 hours for 7 days), and an analgesic was injected intramuscularly (buprenorphine, Temgesic®, Boehringer Mannheim GmbH, Mannheim, Germany; 0.05 mg/kg body weight every 12 hours for 3 days). A follow-up examination was carried out 2 months after surgery under sedation to check if the provisional restorations were still serviceable or had been lost. The animals were sacrificed after 4 months of implant loading with an intravenous injection of 20% solution of pentobarbital (Narcoren, Merian GmbH, Hallbergmoos, Germany) to achieve cardiac arrest. AB from both buccal and lingual sides of the mandibular bone distant at least 5 mm, respectively, from the first (NL) and the last (IL) implants, and the implants together with the surrounding bone were removed and fixated in Schaffer's solution (96% ethanol and 37% formaldehyde, 70:30 v/v) for 24 hours. The specimens were dehydrated in a graded series of ethanol. Thereafter, they were embedded in methylmetacrylate (Technovit®7200, Heraeus Kulzer, Dormagen, Germany). The samples were cut parallel to the longitudinal axis of the implant in a buccal-lingual direction. By the "sawing and grinding" technique they were ground to a thickness of 100 μ m (Exakt Apparatebau GmbH, Norderstedt, Germany). Only the two central sections of each specimen were used for the investigation. The total number of specimens was 20 for IL and AB, and 5 for NL. The number of sections was 40 for IL and AB, and 10 for NL. The number of measurements performed in this study was 200 for IL and AB for both BSE and CPL, and 50 for NL for both BSE and CPL (Table 1).

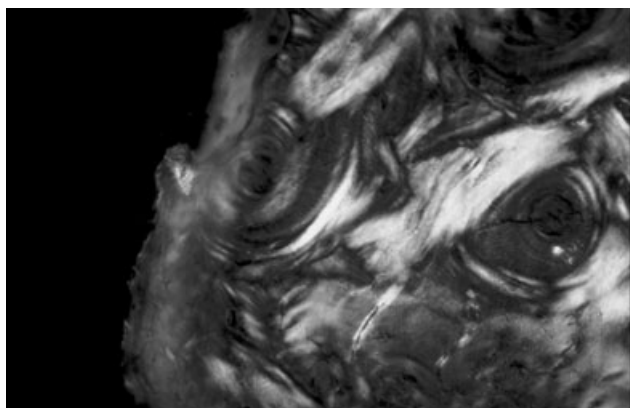


Figure 1 Circularly polarized light microscope (LM) image of the peri-implant bone (immediately loaded) after converting in a gray scale. Transverse collagen fibers appear in gray white. $\times 100$.

Birefringence Analysis

The specimens were analyzed for collagen fiber orientation in an Axiolab light microscope (Zeiss, Oberchen, Germany) equipped with two linear polarizers and two-quarter wave plates arranged to have a transmitted CPL. Collagen fibers aligned transverse to the direction of the light propagation (parallel to the plane of the section) appeared “bright.” The microscope was connected to a high-resolution digital camera (FinePix S2 Pro, Fuji Photo Film Co. Ltd., Minato-Ku, Japan). The measurements were performed on digital images at $50\times$ and $100\times$ after converting them in gray scale at eight bits (Figure 1). For each pixel in the grid, a value between 0 and 255 (0 = black, 255 = white) was assigned. A threshold of gray-value levels (170–250), related to the transverse collagen fiber areas, was made before quantitative analysis (Figure 2) using software Image J, v 1.29 x (National Institutes of Health, at <http://rsb.info.nih.gov/nih-image/>). To ensure accuracy, we calibrated the software for each experimental image. A total of 200 measurements for IL implants, 200 for AB, and 50 for NL implants were made. The analysis considered the areas occupied by transverse collagen fibers (measured in pixel) since they were related to the bone areas subjected more to compressive than to tensile stress like longitudinal collagen fibers. The mean values of all measurements for each group were considered for statistical analysis.

Sample Preparation for Scanning Electron Microscope (SEM) Evaluation

After the preparation of thin section, the resin blocks remaining were polished and coated with a very thin

layer of gold by vacuum evaporation Emitech K 550 (Emitech Ltd, Ashford, Kent, UK). Au sputtering was used rather than C sputtering since it was more easily controlled and reported as a useful method by Bloebaum and colleagues.⁸ The composite specimen blocks were placed on the storage of a SEM (LEO 435 Vp, LEO Electron Microscopy Ltd, Cambridge, UK) equipped with tetra solid-state BSE detector. The BSEs are generated from about a $0.5\text{-}\mu\text{m}$ -thick surface layer of the specimen, and their number is strongly dependent on the atomic number of the specimen, increasing as a function of the atomic number. The resulting BSE signal can be converted into a digital black/white image where the intensity (gray level) of any pixel in the image is proportional to the atomic number of the corresponding location on the target materials. Some of the major problems in the BSE method are the stability of the SEM and the calibration of the BSE signal for mineral concentration values. In particular, when the BSE technique is used to measure the distribution of the mineral density within and between groups of specimens, all factors that may increase the width of the mineral distribution such as intra-assay and inter-assay variances and also interindividual variation have to be evaluated carefully. For these reasons, the specimens must be repeatedly measured during a multi-session analysis using the same operating conditions for the SEM by saving them in the computer memory and restoring them prior to every image capture. SEM operating conditions included 150- to 30-kV accelerating voltage, 14- to 32-mm working distance, and 0.75-nA probe current. The images were captured in the BSE mode with nine



Figure 2 Threshold of Figure 1 used for measuring the collagen fiber orientation. Only the gray level between 170 and 250 was converted in black.

scans using a line average technique. SEM operating conditions were stored in the computer memory and were restored prior to every image capture. Five measurements for each specimen were performed for a total of 200 measurements for IL implants, 200 for AB, and 50 for NL implants. The weighted mean gray level (MGL) of each image was calculated following the equation reported by Bloebaum and colleagues¹⁵:

$$MGL = \sum_{i=6}^{255} \frac{A_i GL_i}{A_t}$$

where A_i = area of i th gray level; GL_i = i th gray level; A_t = total area imaged. This provides a mean value for the backscattered signal, independent of porosity (black pixel = 0–5 in the BSE image). The BSE signal (gray scale) was calibrated using the “atomic number (Z) contrast” of reference materials. Using this method, two different reference materials of known Z were imaged under defined conditions. The BSE images were calibrated using both carbon ($Z = 6$) (gray level 25 ± 1) and aluminium ($Z = 13$) (gray level 255 ± 1) as reported by Roschger and colleagues.¹⁶ Under the same brightness and contrast conditions, the BSE gray level was calibrated for bone calcium concentration values as follows: the BSE gray level of the osteoid (Ca < 0.2%), which showed a gray level of less than 50, was assumed as standard for the lowest mineralized bone matrix, while the BSE gray level of pure hydroxylapatite (with a known stoichiometric content of Ca of 39.86 wt%), which showed a gray level of 200, was used as standard for the highest mineralized bone matrix. All images were analyzed using Image J 1.32j (Wayne Rasband National Institute of Health, Bethesda, Maryland, USA). The weighted MGL of all measurements for each group was considered for statistical analysis.

Statistical Analysis

Statistical analysis was performed using a software package Sigma Stat 3.0 (SPSS Inc., Ekrath, Germany). All the data were checked for normality distribution with Kolmogorov–Smirnov test before evaluation. The z -test comparison of proportions was used to determine if the bone-implant contact (BIC) rate was significantly different in the IL and NL dental implants. The one-way analysis of variance and the Holm–Sidak Test for multiple comparisons were used, respectively, to test the null hypothesis (H_0) between the groups and multi-

TABLE 2 Histomorphometric Analysis

z-Test				
Samples	Size	Proportion	z	p
Immediately loaded implants	20	0.778	−0.592	0.554
5	0.780			

There is no significance in the proportions of individuals for bone-implant contact within the two groups ($p = 0.554$).

Difference of sample proportion = −0.00200; pooled estimate for $p = 0.778$; standard error of difference of sample proportions = 0.208; 95% confidence interval for difference = −0.409–0.405.

comparisons pairwise to determine which groups were different for both the amount of transverse collagen fibers and bone mineral density. For all the tests performed, the confidence level alpha chosen was 5%.

RESULTS

The bone/implant contact ratio (BIC %) was $77.8 \pm 5.9\%$ for IL implants and $78.0 \pm 5.8\%$ for NL implants; the difference was not statistically significant ($p = .554$) (Table 2). Under CPL, transverse collagen fibers, which lie in the plane of the section, appeared bright (gray white), while longitudinal collagen fibers, which ran perpendicular to the plane of the section, appeared dark (dark gray) (Figures 3–6). The areas covered by transverse collagen fibers in the peri-implant bone of IL specimens were $112,453 \pm 4,605$ pixels (mean \pm SD) (see Figures 3 and 4), $87,256 \pm 2,428$ pixels (mean \pm SD) in NL specimens (see Figure 5), and $172,340 \pm 3,892$ pixels (mean \pm SD) in AB specimens (see Figure 6). The difference between groups was statistically significant ($p < .001$) (Table 3 and Figure 7). The AB under CPL appeared mainly formed by osteons (see Figure 6). Under SEM observation, using secondary electrons, the peri-implant bone of IL implants showed less marrow spaces and a more organized bone (Figure 8), while the peri-implant bone of the NL implants appeared rich in marrow spaces and less organized (Figure 9). Using the BSE signal, the different degree of mineralization of the bone matrix appeared in a different gray level. The gray-white areas were related to the high content of the mineral (Figures 10–12). The gray level of the peri-implant bone was 137 ± 19 for IL implants (see Figure 10) and 115 ± 24 for NL implants (see Figure 11), while in the bone 5 mm away from implant surface (AB), the gray level was 125 ± 26 (see

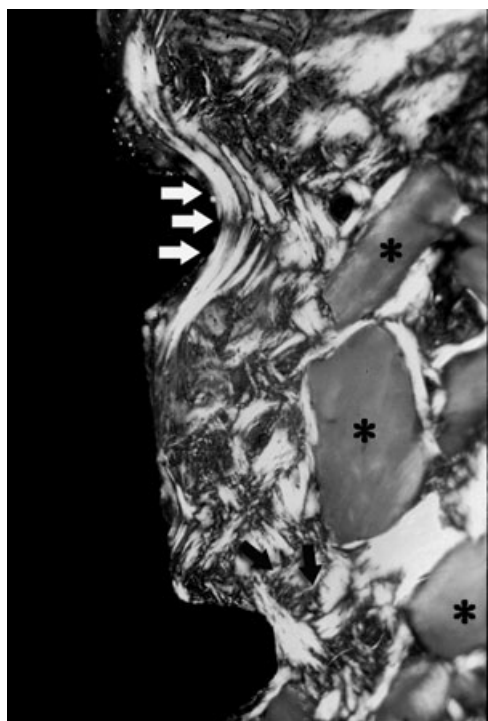


Figure 3 Circularly polarized light LM image of the peri-implant bone of an immediately loaded implant with woven (black arrows) and lamellar (white arrows) appearances. Marrow spaces (*) are present. Transverse collagen fibers appear in gray white. $\times 50$.

Figure 12). The difference among the groups was statistically significant $p < .001$ (Table 4 and Figure 13).

DISCUSSION

The bone loss around dental implants is greater during healing and the first year of function; the possible caus-

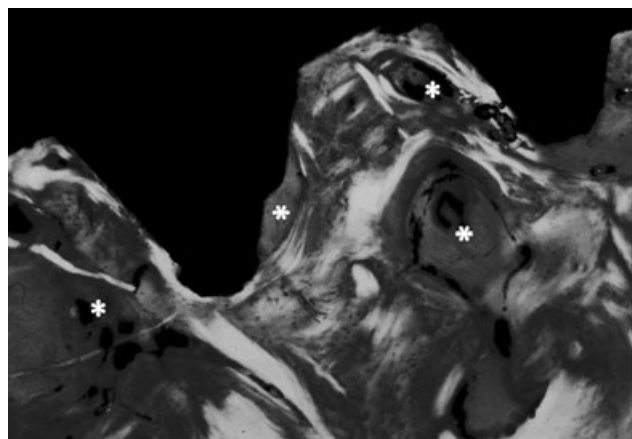


Figure 4 Circularly polarized light LM image of the peri-implant bone of an immediately loaded implant. Transverse collagen fibers, in gray white, are more represented under the lower flank of the implant threads than the upper flank of the implant threads where marrow spaces (*) contact directly the implant surface. $\times 100$.

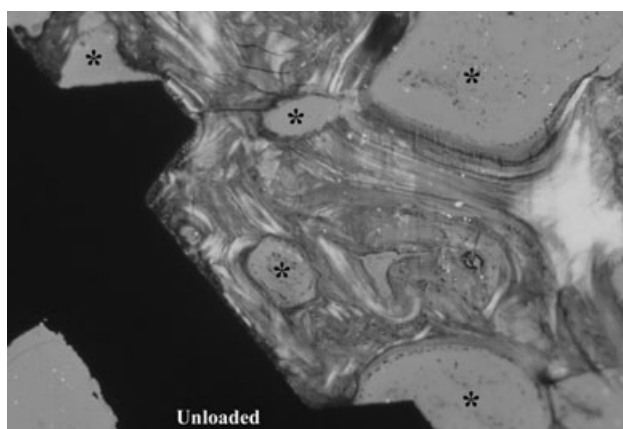


Figure 5 Circularly polarized light LM image of the peri-implant bone of an unloaded implant. Transverse collagen fibers appear in gray white. Many marrow spaces (*) are present. $\times 50$.

ative factors are several and vary from surgical trauma, occlusal overload, and biological width.¹⁷ The implant profiles at microscopic and macroscopic levels are the main stress distributors so they are able to address the physiological response of the bone.¹⁷ Strain is concentrated at the point where bone contacts the tip of the threads. According to Frost,¹⁸ 1,500 to 2,500 $\mu\epsilon$ is the range of “minimum effective strain for mechanically controlled bone remodeling”; above 4,000 $\mu\epsilon$, the bony structure is not able to adapt or repair and, therefore, creep phenomena and fatigue flaw will appear.¹⁹ Moreover, the mechanostat theory claims that if the strain (stress) to which a bone is exposed is lower than 50 to 200 $\mu\epsilon$, a net loss of bone will occur.¹⁸ In the present

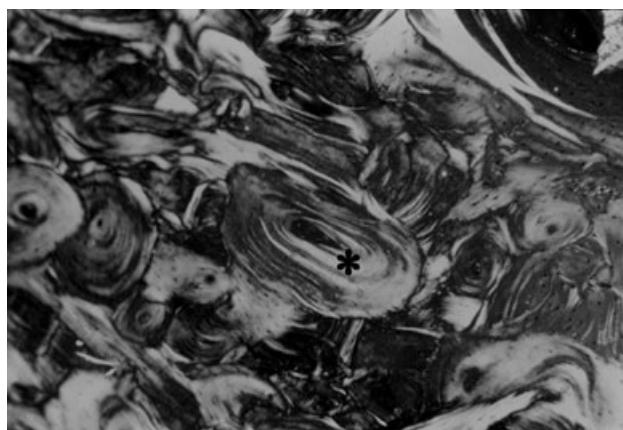


Figure 6 Circularly polarized light LM image of the alveolar bone. Transverse collagen fibers appear in gray white inside a predominantly osteonal bone. A secondary osteon (*) with mainly transverse collagen fibers (gray white) is visible. $\times 100$.

TABLE 3 Statistical Evaluation for Transverse Collagen Fibers

Group Name	ANOVA				
	<i>n</i>	Mean	SD	SEM	
IL bone	200	112,453.000	4,605.000	325.623	
AB	200	172,340.000	3,892.000	275.206	
NL bone	50	87,256.000	2,428.000	343.371	
Source of Variation	<i>df</i>	SS	MS	<i>F</i>	<i>p</i>
Between groups	2	493,777,487,577.777	246,888,743,788.889	14,669.099	<0.001
Residual	447	7,523,248,127.000	16,830,532.723		
Total	449	501,300,735,704.777			
Holm–Sidak Multiple Comparison					
Comparison	Diff. of Means	<i>t</i>	Unadjusted <i>p</i>	Critical level	Significant ?
IL bone versus NL bone	25,197.000	38.845	0.000	0.050	Yes
IL bone versus AB	59,887.000	145.977	0.000	0.025	Yes
AB versus NL bone	85,084.000	131.168	0.000	0.050	Yes

With ANOVA, the differences in the mean values of the areas (pixel) related to transverse collagen fibers among the treatment groups are greater than would be expected by chance; there is a significance ($p = <0.001$, power of performed test with $\alpha = 0.05:1.00$). The multiple comparison procedures (Holm–Sidak method) performed for all pairwise indicate a significance among all the groups. $\alpha = 0.05$. AB = alveolar bone; ANOVA = analysis of variance; *df* = degrees of freedom; IL = immediately loaded; MS = mean of square; NL = unloaded; SEM = scanning electron microscope; SS = sum of square.

study, the IL implants showed both more transverse collagen fibers and mineral density in the peri-implant bone matrix compared with NL implants. Moreover, comparison showed that a different relationship between thread design and birefringent areas related to transverse collagen fibers was evident (see Figures 3 and 4). The transverse collagen fibers appeared more represented under the lower flank in the wide threads, while

in the narrow threads, they were more uniformly distributed. Neither statistical evaluations between upper and lower flank of the threads nor between wide and narrow threads were made since in the first case, a large quantity of marrow spaces in close contact with the

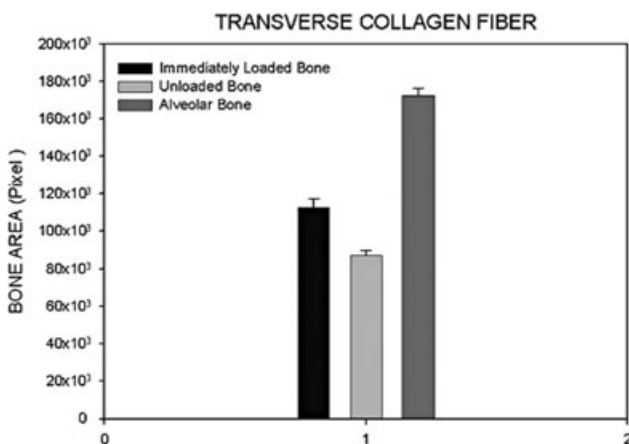


Figure 7 Transverse collagen fibers of the different groups are plotted versus bone area fraction expressed in square pixels.

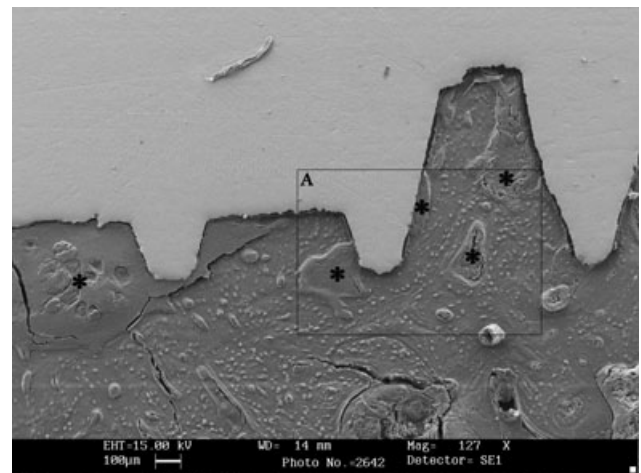


Figure 8 SE image of peri-implant bone of an immediately loaded implant. The bone appears organized since the osteocytes are well distributed and the marrow spaces (*) are few. The rectangle A is investigated with backscattered electron signal and is represented in Figure 13. $\times 127$.

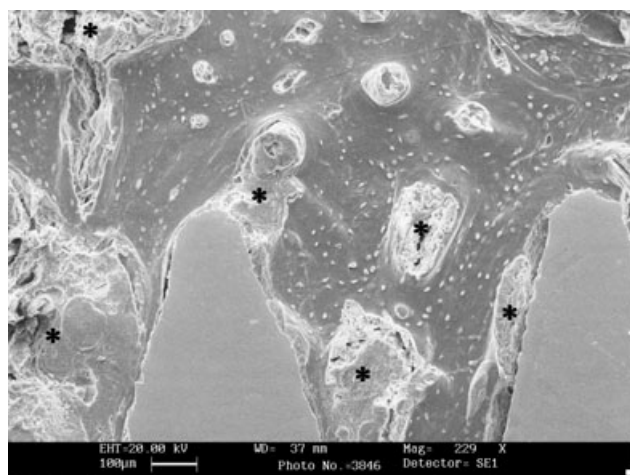


Figure 9 SE image of peri-implant bone of an unloaded implant. The bone appears not organized since the osteocytes are not well distributed and the marrow spaces (*) are more represented. $\times 229$.

implant surface was noted; in the last case, the different position of the threads (one more coronal than the other) determines a different degree of load transmission to the adjacent bone tissue. Furthermore, the narrow threads (0.25 mm) showed an extensive variance of collagen fiber orientation with a predominance of transverse collagen fibers within lamellar bone around the first thread (white arrows) and well-distributed transverse and longitudinal collagen fibers within woven bone around the second thread (black arrows) (see Figure 3). The relation between load direction and collagen fiber orientation should be best addressed in

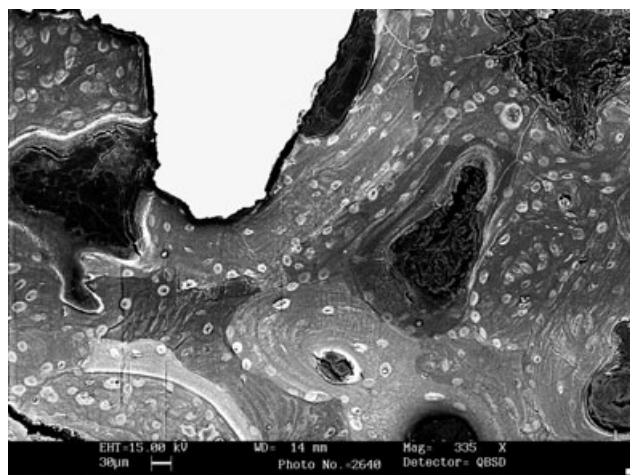


Figure 10 Backscattered electron image of peri-implant bone of an immediately loaded implant. In light gray are the areas with high mineral density. The area of this image is indicated by rectangle A in Figure 11. $\times 335$.



Figure 11 Backscattered electron image of peri-implant bone of an unloaded implant. In light gray are the areas with high mineral density. Marrow space with vessels inside (arrows). $\times 444$.

further research. The collagen fibers in the AB were highly oriented transversally; this is in accordance with the presence of a predominantly bright osteonal arrangement of the bone. Moreover, the mandibular bone of the minipig has a thick circumferentially cortex made of lamellar bone, with a few marrow spaces (see Figure 6), since it is normally subject to high stress. The collagen fibers in the peri-implant bone of IL implants were more oriented transversally than in the peri-implant bone of NL implants. The results could be explained considering the stress/strain distribution in bone due to the threads, which seems to be more

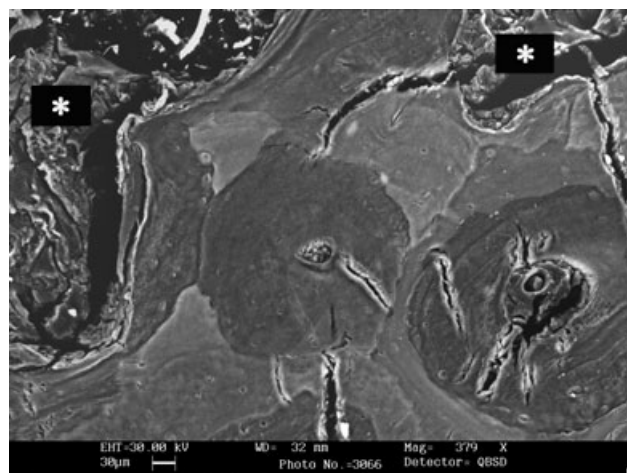


Figure 12 Backscattered electron image of alveolar bone. In light gray are the areas with high mineral density. Marrow spaces (*) are indicated. $\times 379$.

TABLE 4 Statistical Evaluation for Mineral Density					
Group Name	ANOVA				
	<i>n</i>	Mean	SD	SEM	
IL bone	200	125,000	26,000	1.838	
AB	200	137,000	19,000	1.344	
NL bone	50	115,000	24,000	3.394	
Source of Variation	<i>df</i>	SS	MS	<i>F</i>	<i>p</i>
Between groups	2	25,777.778	12,888.889	24.559	<0.001
Residual	447	234,587.000	524.803		
Total	449	260,364.778			
Comparison	Holm–Sidak Multiple Comparison				
	Diff. of Means	<i>t</i>	Unadjusted <i>p</i>	Critical Level	Significant ?
IL bone versus NL bone	22,000	6.074	0.000	0.017	Yes
IL bone versus AB	12,000	5.238	0.000	0.025	Yes
AB versus NL bone	10,000	2.761	0.006	0.050	Yes

With ANOVA, the differences in the mean values of the gray level among the treatment groups are greater than would be expected by chance; there is a significance ($p = <0.001$, power of performed test with $\alpha = 0.05:1.000$). The multiple comparison procedures (Holm–Sidak method) performed for all pairwise indicate a significance among the groups. Alpha = 0.05.

AB = alveolar bone; ANOVA = analysis of variance; *df* = degrees of freedom; IL = immediately loaded; MS = mean of square; NL = unloaded; SEM = scanning electron microscope; SS = sum of square.

favorable to orient the collagen fibers inside the bone matrix especially when they were wide (see Figures 3–5). This statement agrees with the observation that marrow spaces were noted in the IL group mainly closest to the upper flanks of the wide threads while in the NL group, they were more represented and uniformly distributed.

The mineralization level after 4 months of loading was higher around IL dental implants than in the peri-implant bone of NL implants, but was less than AB. This finding is in accordance with the observations reported by several authors^{9,10,19} for a close relation between stress level and mineral density. In the AB, in fact, a high presence of osteons, with transverse collagen fibers highly mineralized (mean of gray value = 137), is correlated with the presence of the high compressive stress areas such as the cortex of the minipig mandible. In the peri-implant bone of NL implants otherwise, the transverse collagen fibers and the mineral density were significantly lower since the implants were not associated with the loading state. The load, in fact, acting in the early phase of osseointegration, produces an increase of transverse collagen fibers and a high level of mineral density. Furthermore, studies in human femoral specimens have demonstrated that transversely oriented collagen fibers are more prevalent in bone areas that are subject to compression.^{20,21} The results of our study are in accordance with Skedros and colleagues,²² who reported that regions subjected to compressive stresses presented a higher mineral density than those subjected to tensile stresses.

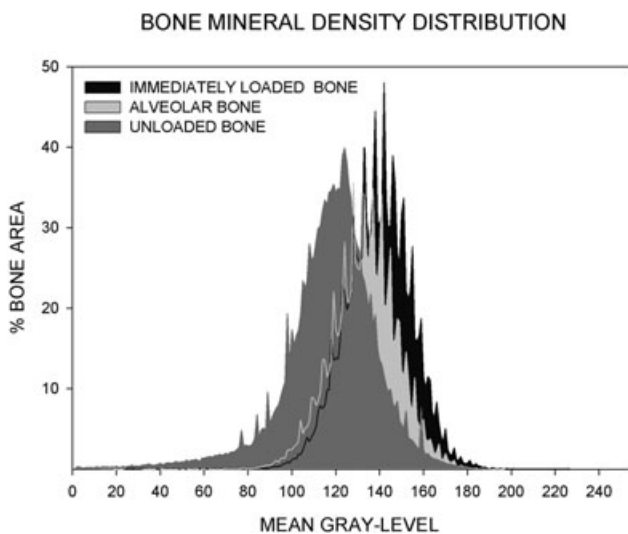


Figure 13 The weighted means of gray level for each group are plotted versus bone area.

The collagen fibers have been implicated in the initiation of matrix calcification with many other matrix proteins including chondrocalcin, proteoglycans, osteonectin, and osteocalcin.²³ The elasticity of bone and thus its resistance to fracture is related to the collagen fiber orientation, to the degree of mineralization, and finally to the water content. Because an increase in stiffness and brittleness of bone tissue follows the replacement of its water content by mineral content, the relationship between mineral content and the strength of bone has been studied extensively.^{24,25} Increasing mineralization density increases the ability of bone to absorb impact energy, although this relationship is not linear; in fact, a very high mineralized bone becomes liable to fracture, since micro-fractures can more readily propagate through bone.⁵ The optimal mineralization density value for bone strength has not yet been determined.²⁶ The immediate loading clinical procedure does not affect the quantity of osseointegration (BIC) but does affect the quality of osseointegration giving rise to a bone matrix rich with highly mineralized transverse collagen fibers.^{27,28} These factors are, most probably, favorable for the maintenance of a mineralized interface of the implants under loading. The results of the present study on collagen fiber orientation are in accordance with our previous study on human samples.^{27,28} In conclusion, our results show that, in minipig mandible, dental implants placed in function immediately after surgery do not present higher BIC than NL implants, but show a significantly higher quantity of highly mineralized transversally oriented collagen fibers.

ACKNOWLEDGMENTS

This work was partially supported by the National Research Council, Rome, Italy; by the Ministry of Education, University, Research, Rome, Italy; and by Research Association for Dentistry and Dermatology, Chieti, Italy.

REFERENCES

- Davies JE. Mechanisms of endosseous integration. *Int J Prosthodont* 1998; 11:391–401.
- Lazzara RJ, Porter SS, Testori T, Galante J, Zetterqvist L. A prospective multicenter study evaluating loading of osseotite implants two months after placement: one-year results. *J Esthet Dent* 1998; 10:280–289.
- Buser D, Nydegger T, Hirt HP, Cochran DL, Nolte LP. Removal torque values of titanium implants in the maxilla of miniature pigs. *Int J Oral Maxillofac Implants* 1998; 13:611–619.
- Nkenke E, Kloss F, Wiltfang J, et al. Histomorphometric and fluorescence microscopic analysis of bone remodelling after installation of implants using an osteotome technique. *Clin Oral Implants Res* 2002; 13:595–602.
- Currey JD. The mechanical consequences of variation in the mineral content of bone. *J Biomech* 1969; 2:1–11.
- Currey JD. The effect of porosity and mineral content on the Young's modulus of elasticity of compact bone. *J Biomech* 1988; 21:131–139.
- Martin RB, Papamichos T, Dannucci DA. Linear calibration of radiographic mineral density using video-digitizing methods. *Calcif Tissue Int* 1990; 47:82–91.
- Bloebaum RD, Skedros JG, Vajada EJ, Bachus KN, Constantz BR. Determining mineral content variations in bone using backscattered electron imaging. *Bone* 1997; 20:485–490.
- Loveridge N, Power J, Reeve J, Boyde A. A bone mineralization density and femoral neck fragility. *Bone* 2004; 35:929–941.
- Skedros JG, Bloebaum RD, Bachus KN, Boyce TM, Constantz B. Influence of mineral content and composition on grey levels in backscattered electron images of bone. *J Biomed Mater Res* 1993; 27:57–64.
- Wang X, Bank RA, TeKoppele JM, Agrawal CM. The role of collagen in determining bone mechanical properties. *J Orthop Res* 2001; 19:1021–1026.
- Portigliatti Barbos M, Bianco P, Ascenzi A, Boyde A. Collagen orientation in compact bone: II. Distribution of lamellae in the whole of the human femoral shaft with reference to its mechanical properties. *Metab Bone Dis Rel Res* 1984; 5:309–315.
- Bromage TG, Goldman HM, McFarlin SC, Warshaw J, Boyde A, Riggs CM. Circularly polarized light standards for investigations of collagen fiber orientation in bone. *Anat Rec* 2003; 274B:157–168.
- Osaki S, Tohno S, Tohno Y, Ohuchi K, Takakura Y. Determination of the orientation of collagen fibers in human bone. *Anat Rec* 2002; 266:103–107.
- Bloebaum RD, Bachus KN, Boyce TM. Backscattered electron imaging: the role in calcified tissue and implant analysis. *J Biomater Appl* 1990; 5:56–85.
- Roschger P, Fratzl P, Klaushofer K, Rodan G. Mineralization of cancellous bone after alendronate and sodium fluoride treatment: a quantitative backscattered electron imaging study on minipigs ribs. *Bone* 1997; 5:393–397.
- Oh TJ, Yoon J, Mish C, Wang HL. The cause of early bone loss: myth or science? *J Periodontol* 2002; 73:322–333.
- Frost HM. Bone "mass" and the "mechanostat" a proposal. *Anat Rec* 1987; 219:1–9.
- Currey JD. The mechanical consequences of variation in the mineral content of bone. *J Biomechanics* 1969; 2:1–11.
- Boyde A, Bianco P, Portigliatti-Barbos M, Ascenzi A. Collagen orientation in compact bone: I. A new method for the

- determination of the proportion of collagen parallel to the plane of compact bone sections. *Metab Bone Dis Rel Res* 1984; 5:299–307.
21. Portigliatti Barbos M, Bianco P, Ascenzi A. Distribution of osteonic and interstitial components in the human femoral shaft with reference to structure, calcification and mechanical properties. *Acta Anat* 1983; 115:178–186.
 22. Skedros JG, Bloebaum RD, Mason MW, Bramble DM. Analysis of a tension/compression skeletal system: possible strain-specific differences in the hierarchical organization of bone. *Anat Rec* 1994; 239:396–404.
 23. Farquharson C, Thorp BH, Whitehead CC, Loveridge N. Alterations in glycosaminoglycan content and sulfation during chondrocyte maturation. *Calcif Tissue Int* 1994; 54:296–303.
 24. Vose GP, Kubala AL. Bone strength—its relationship to X-ray determined ash content. *Hum Biol* 1959; 31:262–270.
 25. Currey JD, Brear K, Zioupos P. The effects of aging and changes in mineral content in degrading the toughness of human femora. *J Biomech* 1995; 29:257–260.
 26. Boyde A, Jones SJ, Noble BS, et al. The effects of estrogen suppression on the mineralization density of iliac crest biopsies in young women as assessed by backscattered electron imaging. *Bone* 1998; 22:241–250.
 27. Traini T, Degidi M, Caputi S, Strocchi R, Di Iorio D, Piattelli A. Collagen fiber orientation in human peri-implant bone of immediately loaded and unloaded titanium dental implants. *J Periodontol* 2005; 76:83–89.
 28. Traini T, Degidi M, Strocchi R, Caputi S, Piattelli A. Collagen fibers orientation near dental implants in human bone: do their organization reflect differences in loading? *J Biomed Mater Res* 2005; 74B:538–546.

Copyright of *Clinical Implant Dentistry & Related Research* is the property of Blackwell Publishing Limited and its content may not be copied or emailed to multiple sites or posted to a listserv without the copyright holder's express written permission. However, users may print, download, or email articles for individual use.